

Exergy flow and energy utilization of direct methanol fuel cells based on a mathematic model

Li Xianglin, He Yaling*, Yin Benhao, Miao Zheng, Li Xiaoyue

State Key Laboratory of Multiphase Flow in Power Engineering, School of Energy and Power Engineering, Xi'an Jiaotong University, Xi'an 710049, China

Received 29 March 2007; received in revised form 31 July 2007; accepted 1 August 2007
Available online 17 August 2007

Abstract

An exergetic analysis model for direct methanol fuel cell (DMFC) is established in the present paper. Expressions of electrical, thermal and total exergetic efficiencies have been deduced with consideration of methanol crossover and over potential in operation. Furthermore, energy utilization of a DMFC system is quantitatively calculated and changes of electrical efficiency and thermal efficiency at various current density, methanol concentration, operating temperature, and cathode pressure have been investigated. Some suggestions of optimal operating conditions of direct methanol fuel cell based on our findings are put forward. Results show that the thermal energy generated in a DMFC takes up a significant amount of exergy in total energy and should be sufficiently used to obtain high total efficiency in a DMFC, high methanol crossover rate is the predominant cause of energy loss when the fuel cell operates at low current density, and total exergetic efficiency of a DMFC reaches its peak value at relatively high current density.

© 2008 Published by Elsevier B.V.

Keywords: Direct methanol fuel cell; Methanol crossover; Exergetic analysis; Model; Efficiency

1. Introduction

A fuel cell is an electrochemical energy-delivery device that converts chemical energy of fuels, typically hydrogen or liquid methanol, into electrical and heat energy without combustion. Not governed by Carnot law, the efficiency of a fuel cell can easily achieve a high level [1]. As a subcategory of proton exchange membrane fuel cell (PEMFC), the direct methanol fuel cell (DMFC) utilizes the liquid methanol solution as its fuel and operates under near room temperature. The DMFC has been identified as the most promising power source for portable and mobile applications on account of its high energy density, simplicity of equipments, low operating temperature, rapid start-up, environmentally benign emissions and so on [2–6].

In spite that the performance of the DMFC has been significantly improved over the last decade, electrical efficiency limitation is still one of the critical problems that hinders the wide application of the DMFC [7,8]. In order to optimize the per-

formance of the DMFC, effects of operating parameters towards electrical exergetic efficiency should be quantitatively analyzed. Furthermore, since large amount of heat is generated due to methanol crossover and irreversible processes in fuel cell operation, analysis of thermal exergetic efficiency could also be useful to increase total efficiency of DMFC systems.

Few literatures about exergetic analysis in fuel cells have been published by far and even fewer papers focus on thermal exergetic efficiency. Ay et al. [9] conducted research about exergetic efficiency at various temperature, anode pressure, and membrane thickness of PEMFC. Ishihara et al. [10] investigated exergetic efficiency of methanol reforming system, they examined exergy flow and compared the efficiency of the total system with that of a single direct methanol fuel cell. Hotz et al. [11] modeled both steam-reformed methanol fuel cell micro-power plant and DMFC micro-power plant and numerical model adopting fourth-order Runge–Kutta method was presented. In all of the above-mentioned studies, the effect of current density has not been taken into account and the operating voltage of the cell and methanol crossover rate have been simplified as constants. Although several researchers have investigated exergetic efficiency of DMFC systems, systematic study on parameters,

* Corresponding author. Tel.: +86 29 82663851; fax: +86 29 82663851.
E-mail address: yalinghe@mail.xjtu.edu.cn (Y. He).

Nomenclature

C	molar concentration (mol L^{-1})
C_p	heat capacity at constant pressure ($\text{J mol}^{-1} \text{K}^{-1}$)
D	diffusivity ($\text{cm}^2 \text{s}^{-1}$)
E_x	molar exergy (kJ mol^{-1})
F	Faraday constant ($96,487 \text{ C mol}^{-1}$)
G_m	molar Gibbs free energy ($\text{kJ mol}^{-1} \text{K}^{-1}$)
H_m	molar enthalpy ($\text{kJ mol}^{-1} \text{K}^{-1}$)
j	current density (A cm^{-2})
j_0	exchange current density (A cm^{-3})
l	length (cm)
n	mole number
N	molar flux ($\text{mol s}^{-1} \text{cm}^{-2}$)
P	pressure (bar)
Q	heat quantity (J)
r_C	methanol crossover rate
S_m	molar entropy ($\text{kJ mol}^{-1} \text{K}^{-1}$)
T	cell temperature ($^{\circ}\text{C}$)
W_e	electric power (W)
x	mass fraction (kg kg^{-1})

Greek

α	reaction order
ε	porosity
η	efficiency
λ	empirical constant in open circuit voltage
ξ	temperature correction coefficient ($\text{J mol}^{-1} \text{K}^{-1}$)

Superscripts

dot (\cdot)	unit time
CO_2	carbon dioxide
elec	electrical
H_2O	water
MEOH	methanol
O_2	oxygen
therm	thermal
total	total

Subscripts

A	anode
C	cathode
ch	chemical
cross	methanol crossover
ex	exergetic value
g	gas
in	inlet
L	exergy loss
l	liquid
lim	limited value
m	molar
n	reference value
out	outlet
ph	physical
sat	saturated value
0	environmental value

which may affect the efficiency of the DMFC, such as methanol concentration, current density, methanol crossover rate, temperature, and pressures has not been reported before.

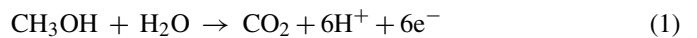
In this study, a method to predict both electrical efficiency and thermal exergetic efficiency has been developed to quantitatively analyze the energy utilization. Based on those analytical equations, the exergetic performance of a DMFC are examined by taking considerations of the effects of parameters such as current density, methanol concentration, operating temperature, and anode pressure. The effect of methanol crossover rate corresponding to various current densities is focused on. Furthermore, suggestions on obtaining optimal practical working conditions are presented based on those findings.

2. Modeling

2.1. Principles of DMFC

As illustrated in Fig. 1, a DMFC typically has a sandwich structure, comprising two flat electrodes and a thin layer of membrane electrode assembly (MEA) in between. As a key component of the DMFC, MEA consists of a catalyst layer and a diffusion layer for both the anode and the cathode side, as well as a polymer-electrolyte membrane.

During operation, methanol solution is fed to the anode electrode, passes through the diffusion layer and reaches the catalyst layer, at which methanol and water molecules are split into electrons and protons and some other species by the following electrochemical reaction:



The generated protons then directly go through the electrolyte to the cathode, meanwhile the electrons, blocked by the proton exchange membrane, have to travel to the cathode via external circuit and form electrical current. At the cathode, the protons and electrons combine electrochemically with oxygen to produce water:



Consequently, the combination of two half-cell reaction is expressed as

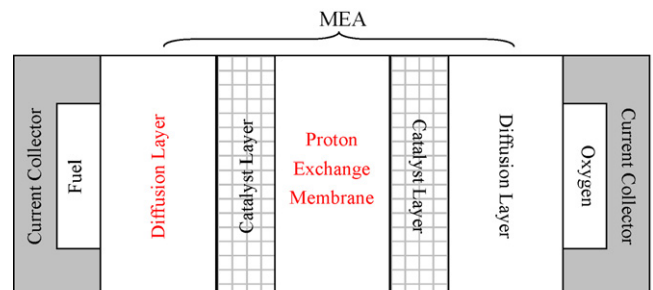
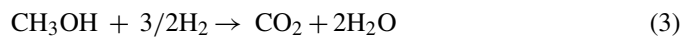


Fig. 1. sketch map of a DMFC.

2.2. Assumptions

In order to simplify the analytical model and examine the effects of principal parameters such as methanol concentration, current density, operating temperature, and operating pressure, the commonly used assumptions in steady state fuel cell models are adopted in this study: all parameters are time-independent, all gases are ideal gases, mass flow is laminar flow, temperature distribution is uniform, kinetic and potential exergy of reactants and productions is neglected, and the amount of water consumed by humidifying air and membrane is neglected. In addition, some special assumptions are made hereafter for the modeling:

- Methanol solution is ideal dilute solution [12] and partial pressure of methanol vapor is neglected.
- Liquid water exists at both anode and cathode, so that partial pressure of water vapor is the saturated pressure corresponding to the operating temperature.
- The methanol crossing over through membrane is completely consumed at cathode [13], and for simplicity, methanol crossover rate was determined only by methanol concentration, current density and geometric size of the cell.
- Pure oxygen rather than air is used as oxidant at cathode and the partial pressure of N_2 and CO_2 at cathode can be neglected.
- The model is one-dimensional to obtain a correlation equation predicting the operating voltage in terms of current density [14].

3. Exergetic efficiency

3.1. Exergy balance

Taking mass, work and thermal exergy into consideration, we can write the general exergy balance equation of a system as follows [15]:

$$\sum \dot{E}_{x,in} = W_e + \dot{E}_{x,therm} + \sum \dot{E}_{x,out} + \dot{E}_{x,L} \quad (4)$$

where $\sum \dot{E}_{x,in}$ is the total exergy in-flow rate by mass and heat flow, W_e the electric power generated by the system, $\dot{E}_{x,therm}$ the thermal exergy generation rate of the system, $\sum \dot{E}_{x,out}$ the total exergy out-flow rate results from mass flow of products, and $\dot{E}_{x,L}$ is the rate of exergy loss of the system. Therefore, the difference between $\sum \dot{E}_{x,in}$ and $\sum \dot{E}_{x,out}$ is the energy consumption rate during operation.

The evaluation of the performance of a DMFC system mainly focuses on its electrical efficiency because fuel cells are used to convert chemical energy of fuel into electricity. At the same time, thermal energy generated during fuel cell system operation also covers a great part of the total energy and should be quantitatively evaluated. Since exergetic efficiency is defined as the ratio of exergy input and output, expressions of thermal exergetic efficiency (η_{ex}^{therm}), electrical efficiency (η_{ex}^{elec}), and total exergetic efficiency (η_{ex}^{total}) are

$$\eta_{ex}^{therm} = \frac{\dot{E}_{x,therm}}{\sum \dot{E}_{x,in} - \sum \dot{E}_{x,out}} \quad (5)$$

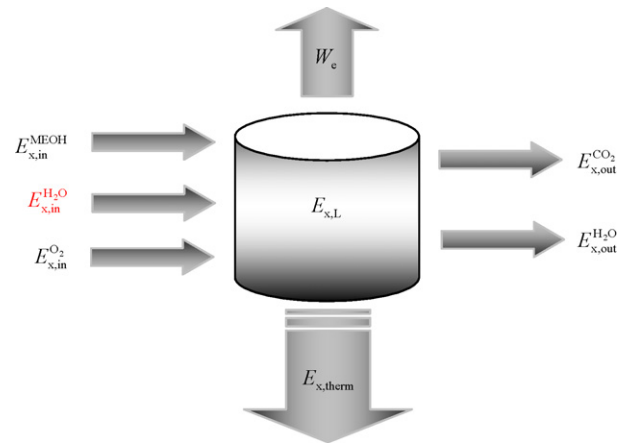


Fig. 2. Exergy flow of a DMFC system.

$$\eta_{ex}^{elec} = \frac{W_e}{\sum \dot{E}_{x,in} - \sum \dot{E}_{x,out}} \quad (6)$$

$$\eta_{ex}^{total} = \frac{W_e + \dot{E}_{x,therm}}{\sum \dot{E}_{x,in} - \sum \dot{E}_{x,out}} \quad (7)$$

3.2. Expressions of efficiency

As discussed above, in a DMFC system, the system exergy inflow results from the mass input of methanol, water, and oxygen and the system exergy outflow results from thermal flow and mass flow due to the output of carbon dioxide and water. By applying general exergy balance of a system to a DMFC system, diagram of the exergy flow of a DMFC is plotted in Fig. 2 and Eq. (4) is rewritten as

$$\dot{E}_{x,in}^{MEOH} + \dot{E}_{x,in}^{H_2O} + \dot{E}_{x,in}^{O_2} = \dot{E}_{x,out}^{CO_2} + \dot{E}_{x,out}^{H_2O} + W_e + \dot{E}_{x,therm} + \dot{E}_{x,L} \quad (8)$$

By substituting the exergy flow rate with the product of molar flow rates \dot{n} and the molar exergy E_x of each species, the exergy balance equation is finally expressed as

$$\dot{n}_{in}^{MEOH} E_x^{MEOH} + \dot{n}_{in}^{H_2O} E_x^{H_2O} + \dot{n}_{in}^{O_2} E_x^{O_2} = \dot{n}_{out}^{CO_2} E_x^{CO_2} + \dot{n}_{out}^{H_2O} E_x^{H_2O} + W_e + \dot{E}_{x,therm} + \dot{E}_{x,L} \quad (9)$$

Since the phenomenon of methanol crossover not only increases cathode polarization but also lowers fuel utilization [16,17], molar flow rates of different species based on stoichiometric relationships in Eqs. (1) and (2) are expressed as follows:

$$\dot{n}_{in}^{MEOH} = \frac{j}{6F(1-rc)} \quad (10)$$

$$\dot{n}_{in}^{H_2O} = \frac{j}{6F(1-rc)} \quad (11)$$

$$\dot{n}_{in}^{O_2} = \frac{j}{4F(1-rc)} \quad (12)$$

$$\dot{n}_{\text{out}}^{\text{H}_2\text{O}} = \frac{j}{2F(1-r_C)} \quad (13)$$

$$\dot{n}_{\text{out}}^{\text{CO}_2} = \frac{j}{6F(1-r_C)} \quad (14)$$

where j is current density and r_C is the methanol crossover rate which determines utilization rate of methanol.

Although methanol crossover deteriorates fuel cell performance, which will be discussed later in voltage–current relationship, heat source generation is increased because the crossed methanol is directly burnt at cathode. Based on the fact that energy of the fuel can be released in form of thermal and electric energy by direct burning of the crossed methanol at cathode and electrochemical reaction at both anode and cathode, thermal energy can be determined by subtracting electrical energy from total energy. Consequently, thermal exergy generation rate is expressed as

$$\begin{aligned} \dot{E}_{x,\text{therm}} = & \left(1 - \frac{T_0}{T}\right) \dot{n}_{\text{in}}^{\text{MEOH}} \\ & \times [r_C \Delta H_m + (1-r_C)(\Delta H_m - \Delta H_{e,m})] \end{aligned} \quad (15)$$

where ΔH_m is total enthalpy difference of reaction, or total energy that could possibly be released, and $\Delta H_{e,m}$, which equals $W_e/\dot{n}_{\text{in}}^{\text{MEOH}}$, is the enthalpy difference released in form of electric energy.

Based on the assumption that the current density is uniform in the cell, the electric power can be simply expressed as

$$W_e = V(j)j \quad (16)$$

By combining Eqs. (5)–(16), the thermal exergetic efficiency, electrical efficiency, and total exergetic efficiency in Eqs. (5)–(8) can be rewritten as

$$\eta_{\text{ex}}^{\text{therm}} = \frac{(1 - (T_0/T)) \cdot [(\Delta H_m - 6FV(j)) + r_C 6FV(j)]}{E_{x,\text{in}}^{\text{MEOH}} + (3/2)E_{x,\text{in}}^{\text{O}_2} + E_{x,\text{in}}^{\text{H}_2\text{O}} - E_{x,\text{out}}^{\text{CO}_2} - 3E_{x,\text{out}}^{\text{H}_2\text{O}}} \quad (17)$$

$$\eta_{\text{ex}}^{\text{elec}} = \frac{6F(1-r_C)V(j)}{E_{x,\text{in}}^{\text{MEOH}} + (3/2)E_{x,\text{in}}^{\text{O}_2} + E_{x,\text{in}}^{\text{H}_2\text{O}} - E_{x,\text{out}}^{\text{CO}_2} - 3E_{x,\text{out}}^{\text{H}_2\text{O}}} \quad (18)$$

$$\eta_{\text{ex}}^{\text{total}} = \frac{(1 - (T_0/T))\Delta H_m + (1-r_C)(T_0/T)6FV(j)}{E_{x,\text{in}}^{\text{MEOH}} + (3/2)E_{x,\text{in}}^{\text{O}_2} + E_{x,\text{in}}^{\text{H}_2\text{O}} - E_{x,\text{out}}^{\text{CO}_2} - 3E_{x,\text{out}}^{\text{H}_2\text{O}}} \quad (19)$$

Molar exergy of each species (E_x), methanol crossover rate (r_C), and operating voltage (V) involved in Eqs. (17)–(19) must be firstly determined to quantitatively calculate thermal

exergetic efficiency, electrical efficiency, and total exergetic efficiency, so that determination of these parameters will be discussed in Sections 2.3–2.5, respectively.

3.3. Molar exergy

Since both kinetic and potential exergy of reactants and products are neglected in this paper, total molar exergy of each species only consists of physical and chemical exergy:

$$E_x = E_{x,\text{ph}} + E_{x,\text{ch}} \quad (20)$$

Physical exergy and chemical exergy can be obtained from [15]:

$$E_{x,\text{ph}} = \int_{T_n}^T C_p \left(1 - \frac{T_0}{T}\right) dT \quad (21)$$

and

$$E_{x,\text{ch}} = E_{x,\text{ch}}^n - \xi(T - T_n) + R_g T_0 \ln x \quad (22)$$

where T_0 is the ambient temperature (298.15 K), T_n the reference temperature (also 298.15 K), T the operating temperature, $E_{x,\text{ch}}^n$ the chemical exergy under reference condition, ξ the temperature correction coefficient used to correct the temperature difference between reference temperature and operating temperature, x the molar fraction, and C_p is the specific heat at constant pressure. Thermodynamic parameters of reactants and products are listed in Table 1.

Based on the assumptions that methanol solution is an ideal dilute solution and fractional pressures of water vapor at both cathode and anode equal to their saturated values corresponding to the operating temperatures, the molar fraction (x) of every reactants and products can be expressed as

$$x^{\text{MEOH}} = \frac{C^{\text{MEOH}}}{C^{\text{H}_2\text{O}} + C^{\text{MEOH}}} = \frac{C^{\text{MEOH}}}{C^{\text{H}_2\text{O}}} = \frac{18C^{\text{MEOH}}}{\rho^{\text{H}_2\text{O}}} \quad (23)$$

$$x^{\text{O}_2} = \frac{P_C - P_{\text{sat}}^{\text{H}_2\text{O}}(T)}{P_C} \quad (24)$$

$$x^{\text{CO}_2} = \frac{P_A - P_{\text{sat}}^{\text{H}_2\text{O}}(T)}{P_A} \quad (25)$$

$$x_A^{\text{H}_2\text{O}} = \frac{P_{\text{sat}}^{\text{H}_2\text{O}}(T)}{P_A} \quad (26)$$

$$x_C^{\text{H}_2\text{O}} = \frac{P_{\text{sat}}^{\text{H}_2\text{O}}(T)}{P_C} \quad (27)$$

Table 1
Thermodynamic parameters of reactants and products [11]

Species	ξ (J mol ⁻¹ K ⁻¹)	$C_{p,m}$ (J mol ⁻¹ K ⁻¹)	S_m^n (J mol ⁻¹ K ⁻¹)	ΔG_f^n (kJ mol ⁻¹ K ⁻¹)	$E_{x,m,\text{ch}}^n$ (kJ mol ⁻¹ K ⁻¹)
Methanol (l)	-33.26	45.42	126.36	-166.43	717.19
O ₂	13.22	29.34	205.16		
CO ₂	-147.28	37.13	213.78	-394.65	20.138
H ₂ O (g)	-118.78	33.57	188.82	-228.75	
H ₂ O (l)	-	75.15	69.98	-237.35	-

Table 2
Parameters used to determine methanol crossover rate [19]

Parameters	Symbol	Anode	Cathode
Membrane thickness	l_m	0.0206 cm	0.0206 cm
Thickness of baking layer	l_b	0.03 cm	0.03 cm
Concentration of reactants in channel	C_h	$0.5 \times 10^{-3} \text{ mol cm}^{-3}$	$0.199 \times 10^{-3} \text{ mol cm}^{-3}$
Diffusion coefficient of methanol in membrane	D_m	$1.0 \times 10^{-5} \text{ cm}^2 \text{ s}^{-1}$	$1.0 \times 10^{-5} \text{ cm}^2 \text{ s}^{-1}$
Diffusion coefficient of methanol in backing layer	D_b	$1.8 \times 10^{-5} \text{ cm}^2 \text{ s}^{-1}$	$0.9 \times 10^{-3} \text{ cm}^2 \text{ s}^{-1}$
Drag coefficient	n_d	3.16	3.16

where saturated pressure $P_{\text{sat}}^{\text{H}_2\text{O}}$ (atm) of water corresponding to local temperature T ($^\circ\text{C}$) is given by [18]:

$$\log P_{\text{sat}}^{\text{H}_2\text{O}} = -2.1794 + 0.02953T - 9.1837 \times 10^{-5}T^2 + 1.4454 \times 10^{-7}T^3 \quad (28)$$

Combining Eqs. (20)–(28), the total molar exergy of each species under specified temperature and pressure can be obtained.

3.4. Methanol crossover rate

To quantitatively examine the effect of methanol crossover and utilization rate of fuel, the methanol crossover rate is defined as

$$r_C = \frac{N_{\text{cross}}}{N_{\text{cross}} + j/6F} \quad (29)$$

where N_{cross} is molar crossover flux and $j/6F$ represents the methanol flux consumed by electrochemical reaction with current density j .

Based on the representation of the methanol crossover flux in Ref. [19]:

$$N_{\text{cross}} = \frac{j_{\text{lim}}^a}{6F} \left(\frac{\beta + n_d j/j_w}{1 + \beta + n_d j/j_w} \right) \left(1 - \frac{j}{j_{\text{lim}}^a} \right) \quad (30)$$

we can rewrite Eq. (29) as

$$r_C = \frac{(j_{\text{lim}}^a - j)(\beta + n_d(j/j_w))}{(j + j_{\text{lim}}^a)(\beta + n_d(j/j_w))} \times 100\% \quad (31)$$

where

$$j_{\text{lim}}^a = 6F \frac{D_b^a C_h^a}{l_b^a}, \quad \beta = \frac{D_m^a l_b^a}{D_b^a l_m^a} \quad (32)$$

and the equivalent current density, j_w , is related to geometric parameters:

$$j_w = \left(\frac{F}{18} \right) \left(\frac{D_b^a}{l_b} \right) \quad (33)$$

Values of parameters to determine crossover rate are summarized in Table 2.

3.5. Operating voltage versus current density

Although the ideal open circuit voltage (OCV) of a DMFC system is 1.21 V [1], the working voltage is considerably lower

than this ideal value in practical operation mainly due to four irreversibilities: fuel crossover, activation loss, ohmic loss, and mass transport loss. Considering these irreversibilities, the empirical relationship of working voltage and current density is [20]:

$$V(j) = V_{\text{oc}} - jR - \left| \frac{RT}{\alpha n F} \ln \frac{j}{j_0} \right| - \left| \frac{RT}{n F} \ln \left(1 - \frac{j}{j_{\text{lim}}} \right) \right| \quad (34)$$

Practical OCV (V_{oc}) in Eq. (34), which takes the effect of methanol crossover into account, can be expressed as [14]:

$$V_{\text{oc}} = 1.2 \times (1 - \lambda) + \frac{RT}{F} \times \ln \left\{ k^*(T)(C_{\text{MEOH}})^{1-(1/\lambda)} \left(\frac{P_{\text{CO}_2, \text{a}}}{P^n} \right)^{-1} \left(\frac{P_{\text{O}_2, \text{c}}}{P^n} \right)^{3/2} \right\} \quad (35)$$

then the relation between working voltage and current density will be obtained as

$$V(j) = 1.2 \times (1 - \lambda) + \frac{RT}{F} \times \ln \left\{ k_{21}^*(T)(C_{\text{MEOH}})^{1-(1/\lambda)} \left(\frac{P_{\text{CO}_2, \text{a}}}{P^n} \right)^{-1} \left(\frac{P_{\text{O}_2, \text{c}}}{P^n} \right)^{3/2} \right\} - j \frac{\delta_m}{\sigma_m} - \frac{RT}{n_A \alpha_A F} \ln \left(\frac{j}{j_{0, \text{A}}} \right) - \frac{RT}{n_C \alpha_C F} \ln \left(\frac{j}{j_{0, \text{C}}} \right) + \frac{RT}{n_{\text{Mixed}} F} \ln \left(1 - \frac{j}{j_{\text{lim}}} \right) \quad (36)$$

The values of parameters in Eq. (36) are summarized in Table 3.

To validate the U – I relationship, the comparison between the predicted value by our model predictions with experimental data of Scott et al. [21] is shown in Fig. 3. As can be seen, the agreement between theoretically predicted values and experimental data is quite good.

Thermal exergetic efficiency, electrical efficiency, and total exergetic efficiency can be investigated with the help of the molar exergy of each species, the methanol crossover rate, and the operating voltage by further analysis will be conducted based on Eqs. (17)–(19).

Table 3
Parameters used to obtain operating voltage vs. current density

Parameters	Symbol	Value	Reference
Faraday constant	F	$96,487 \text{ C mol}^{-1}$	
Gas constant	R	$8.314 \text{ J mol}^{-1} \text{ K}^{-1}$	
Reference pressure	P^0	1.0 bar	
Methanol concentration in channel	C_{MEOH}	$0.5 \times 10^{-3} \text{ mol cm}^{-3}$	
Number of electrons in methanol oxidation	n_{MEOH}	6	
Number of electrons in anode reaction	n_A	6	
Number of electrons in cathode reaction	n_C	4	
Limiting current density of anode	j_{lim}	$n_{\text{MEOH}}F \times 10^{-5} \times \varepsilon^{1.5} \times C_{\text{MEOH}} \times 10^4 \text{ mA m}^{-2}$	Scott et al. [14]
Exchange current density of anode	$j_{0,A}$	$1.08 \times 10^{-21} \times \exp(0.086T) \text{ mA m}^{-2}$	Berning [22]
Exchange current density of cathode	$j_{0,C}$	$5.04 \times 10^{-21} \times \exp(0.086T) \text{ mA m}^{-2}$	Assumed
Empirical constant	λ	0.56	Scott et al. [14]
Empirical constant	k^*	$2.4 \times 10^3 \times \exp[-5.83 \times 10^3 \times (1/T - 1/363.15)]$	Scott et al. [14]
Liquid volume fraction	ε	0.6–0.8	Scott et al. [14]
Mixed coefficient of concentration polarization	n_{Mixed}	1.2	Fitting parameter
Electron transfer coefficient in anode	α_A	0.5	Scott et al. [14]
Electron transfer coefficient in cathode	α_C	0.92	Scott et al. [14]
Thickness of Nafion membrane	δ_m	175 μm	Nafion 117
Conductivity of Nafion membrane	σ_m	0.01 S cm^{-1}	Scott et al. [13]

4. Results and discussion

4.1. Effect of current density

Fig. 4 shows the variation of electrical efficiency, thermal exergetic efficiency, and total exergetic efficiency with current density for a DMFC at 90 °C, 1.0 bar anode pressure and 3.0 bar cathode pressure. There is a maximum in total exergetic efficiency with the current density around 87 mA cm⁻² and the maximum efficiency reaches 36.6%. Based on Eq. (19), this maximum of total exergetic efficiency is due to the trade-offs between methanol crossover rate and operating voltage. The variation of methanol crossover rate and operating voltage with current density is illustrated in Fig. 5. As can be seen in Fig. 5, at low current density, the methanol crossover rate sharply decreases with increasing current density and more energy stored in methanol is released by electrochemical reac-

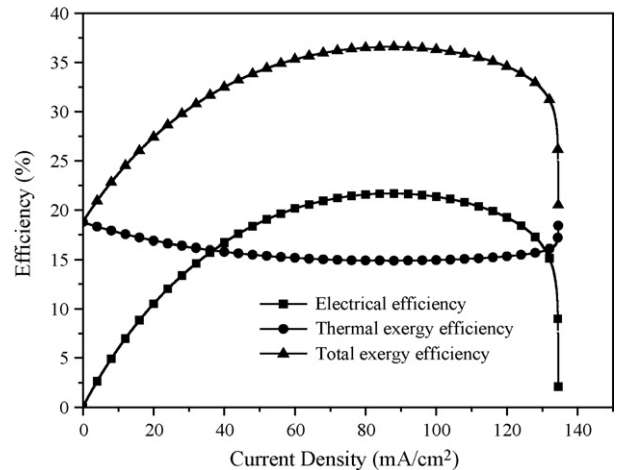


Fig. 4. Different efficiencies vs. current density (anode pressure 1.0 bar, cathode pressure 3.0 bar, methanol concentration 0.5 mol L⁻¹, and temperature 90 °C).

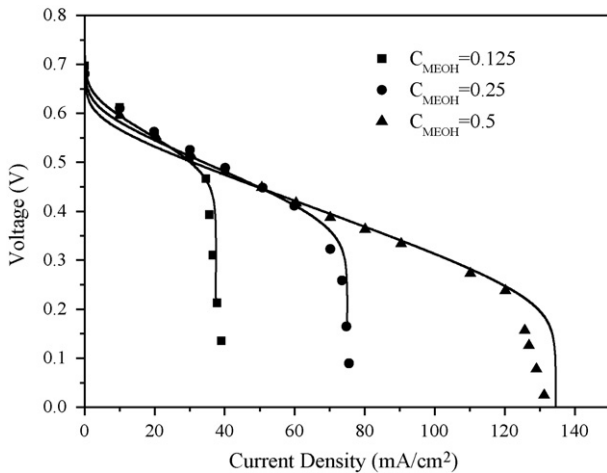


Fig. 3. Comparison between model predictions and experimental data [21] with different methanol concentrations (anode pressure 1.0 bar, cathode pressure 1.5 bar, and temperature 90 °C).

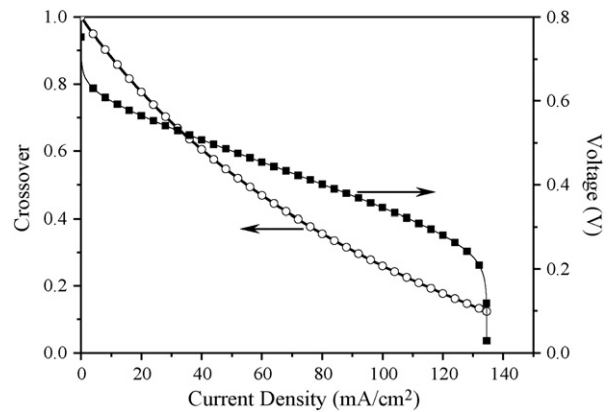


Fig. 5. The crossover rate and operating voltage vs. current density (anode pressure 1.0 bar, cathode pressure 3.0 bar, methanol concentration 0.5 mol L⁻¹, and temperature 90 °C).

tion rather than combustion, so that the total exergetic efficiency increases with increasing current density. However the rapid decrease of operating voltage with increasing current density, or the rapid increase of the over-potential of the cell, significantly reduces the total exergetic efficiency at high current density.

Fig. 4 also presents the comparison between electrical efficiency and thermal exergetic efficiency. With the current density of 87 mA cm^{-2} , electrical efficiency reaches its maximum value of 21.7%, while, thermal exergetic efficiency reaches its minimum value of 14.9% with the same current density. As also can be seen in Fig. 4, at low current density and around limiting current density, the thermal exergetic efficiency is even higher than electrical efficiency. Therefore, cascade utilization of energy by heat and electrical cogeneration or combined cooling, heat, and power systems should be promoted to make full use of the energy storage in fuel and thus increase the exergetic efficiency of the fuel cell system.

4.2. Effect of methanol concentration

Fig. 6 shows variations of total exergetic efficiency with current density with different methanol concentrations, at 90°C , 1.0 bar anode pressure and 3.0 bar cathode pressure. As can be seen in Fig. 6, total exergetic efficiencies at any methanol concentration reaches maximum values at certain current densities: maximum efficiency is 49.7% at current density of 33 mA cm^{-2} for 0.125 mol L^{-1} methanol, 44.1% at current density of 60 mA cm^{-2} for 0.25 mol L^{-1} methanol, and 21.7% at current density of 87 mA cm^{-2} for 0.5 mol L^{-1} methanol. Based on Fig. 6, it is obvious that the lower the methanol concentration, the higher the maximum efficiency could be yielded during fuel cell operation.

The cell could yield higher exergetic efficiency during operation using lower concentration methanol resulted from two aspects: low methanol crossover rate and high operating voltage at a certain current density. Comparison of methanol crossover rate and operating voltage with current density with different methanol concentrations are shown in Fig. 7. As can be seen

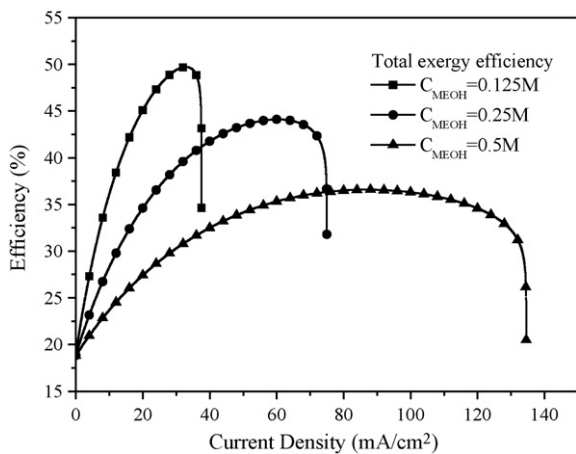


Fig. 6. The total exergetic efficiency vs. current density with different methanol concentration (anode pressure 1.0 bar, cathode pressure 3.0 bar, and operating temperature 90°C).

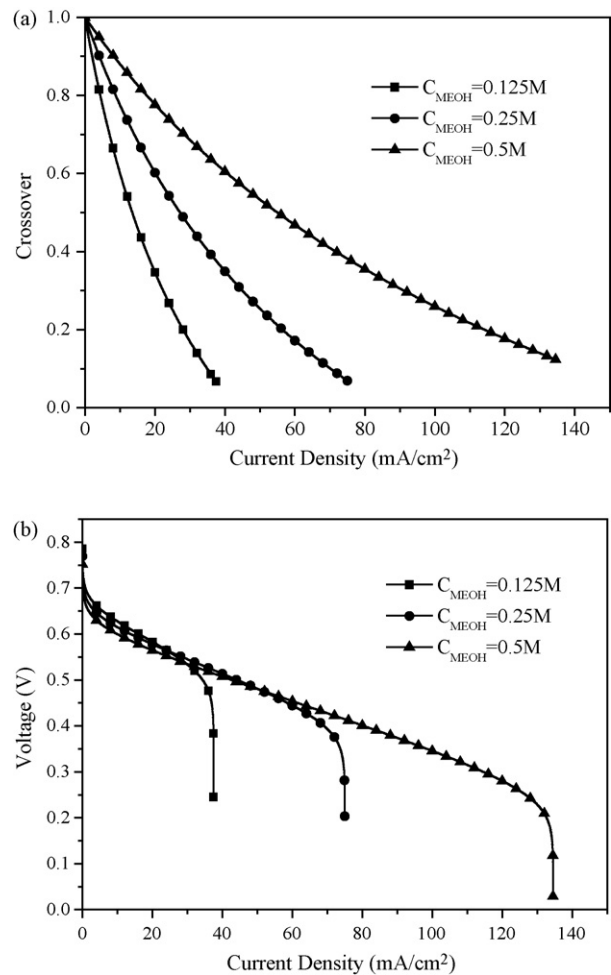


Fig. 7. The variation of parameters with different methanol concentration (anode pressure 1.0 bar, cathode pressure 3.0 bar, and temperature 90°C): (a) the methanol crossover rate vs. current density and (b) the operating voltage vs. current density.

in Fig. 7a and b, the methanol crossover rate decreases more rapidly with increasing current density for low methanol concentration than for high methanol concentration, also operating voltage of cell for low concentration methanol is slightly higher than that for high methanol concentration due to higher OCV based on Eq. (35).

4.3. Effect of cathode pressure

Fig. 8 represents the variation of total exergetic efficiency of a DMFC with different cathode pressures, at 90°C and 1.0 bar anode pressure. As can be seen in Fig. 8, at a certain current density, total exergetic efficiency increases with increasing cathode pressure, and maximum efficiency increases with increasing cathode pressure from 34.6% at 1.0 bar to 36.6% at 3.0 bar.

The increase of cathode pressure leads to both advantageous and disadvantageous effects on fuel cell operation. On one hand, total exergetic efficiency is high at high cathode pressure; on the other hand, high cathode pressure not only brings about more challenges on properties of electrolyte membrane, seal of fuel cell, and performance of auxiliary equipments but also is adverse

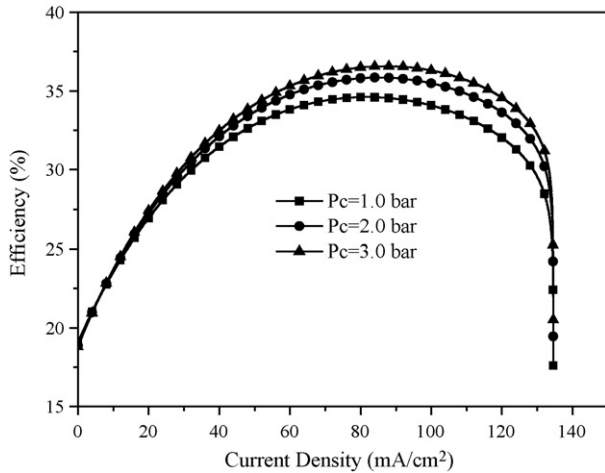


Fig. 8. The total exergetic efficiency vs. current density with different cathode pressures (anode pressure 1.0 bar, methanol concentration 0.5 mol L^{-1} , and temperature 90°C).

to the stability and durability of the fuel cells. It is interesting to notice from Fig. 8 that the maximal total exergetic efficiency only slightly increases from 35.9% to 36.6% when cathode pressure increases from 2.0 to 3.0 bar. According to Eqs. (19) and (35), the trend of increase of total exergetic efficiency decreases with the increase of cathode pressure, in other words, under relatively high cathode pressure, the benefit of further increasing cathode pressure is rather limited and the cost will significantly increase. Therefore, the trade-off between efficiency of fuel cell systems and their cost needs to be considered in practical operation.

4.4. Effect of temperature

The variations of total exergetic efficiency, electrical efficiency, and thermal exergetic efficiency of a DMFC with operating temperatures at 1.0 bar anode pressure and 3.0 bar cathode pressure are presented in Fig. 9. It can be seen in Fig. 9a that total exergetic efficiency rapidly increases with increasing temperature, the maximum efficiencies at 70, 80, and 90°C are 29.2, 32.9, and 36.6%, respectively. The increase of total exergetic efficiency with increasing temperature results from the increase of both electrical efficiency and thermal exergetic efficiency with increasing temperature as is illustrated in Fig. 9b. According to Eqs. (35) and (18), at a given current density, the increase of temperature will heighten cell voltage and consequently increase the electrical efficiency. Also the increase of temperature will heighten thermal exergy of a given amount of heat based on the second law of thermodynamics, thereby improves the thermal exergetic efficiency.

It is also interesting to notice from Fig. 9a that the increase of total exergetic efficiency with increasing temperature is the most rapid around medial current density. According to Fig. 9b, the increase of thermal exergetic efficiency with temperature is found almost uniform at any current density except around limiting current density. However, significant increase of electrical efficiency with temperature could only be observed around media current density because the increase of electrical effi-

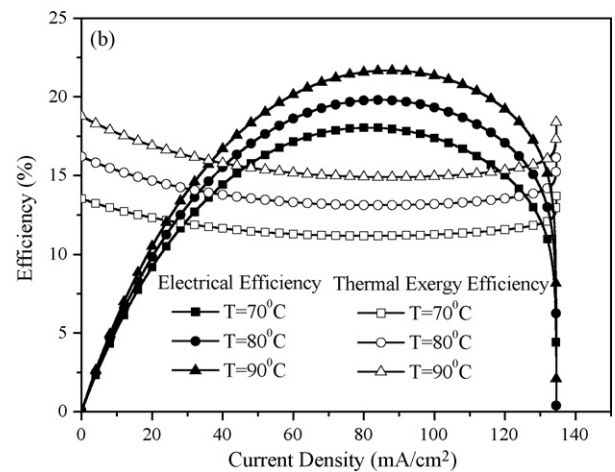
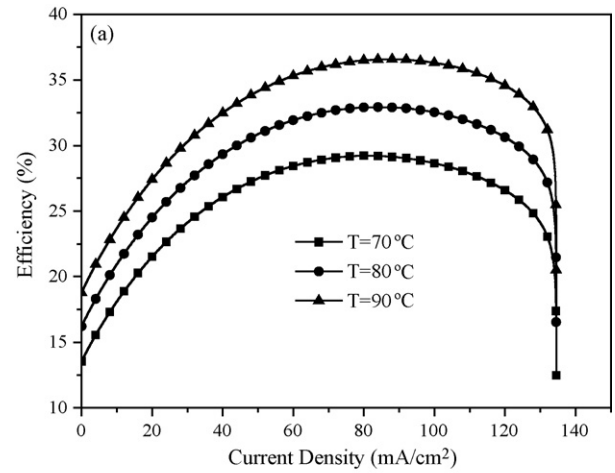


Fig. 9. Different efficiencies vs. current density at different operating temperature (anode pressure 1.0 bar, cathode pressure 3.0 bar, and methanol concentration 0.5 mol L^{-1}): (a) the total exergetic efficiency and (b) electrical efficiency and thermal exergetic efficiency.

ciency is markedly weakened by both high methanol crossover rate at low current density and limited increase of operating voltage around limiting current density.

5. Conclusion

In this paper, expressions of thermal exergetic efficiency, electrical efficiency, and total exergetic efficiency have been developed to quantitatively analyze the energy utilization and transfer in a DMFC. Based on Eqs. (17)–(19), effects of parameters such as current density, methanol concentration, operating temperature, and cathode pressure on fuel cell efficiency are studied. Primary findings and conclusions are summarized below:

1. The energy generated by a DMFC is composed of electric energy and thermal energy, since large quantity of thermal energy is generated in fuel cell operation, thermal exergetic efficiency takes up a significant part of total efficiency, especially at low current density. In order to improve the overall efficiency of a single DMFC or integrated fuel cell stacks,

thermal exergy generated during operation should be fully used.

2. In terms of total exergetic efficiency, the DMFC could achieve better performance for relatively high current density since methanol crossover rate is depressed.
3. Both electrical efficiency and total exergetic efficiency reaches maximum values at any methanol concentrations, and maximum electrical efficiency and total exergetic efficiency appear at relatively high current density. The DMFC could yield higher efficiency using low concentration methanol than that using high concentration methanol because of the lower methanol crossover rate and higher open circuit voltage.
4. The efficiency of the DMFC could be heightened by increasing cathode pressure, however, the increase of efficiency is very limited if the cathode pressure has already been high. Furthermore, the increase in cathode pressure brings about more challenges on fabrication, sealing, and maintenance of fuel cell stacks, increases investments of auxiliary devices such as air feed instruments and pipelines, and makes against life time of fuel cells. Take both cost and efficiency into consideration, cathode pressure should not be too high during fuel cell operation.
5. Total exergetic efficiency of a DMFC could be significantly increased by increasing temperature due to the improvements of both electrical efficiency and thermal exergetic efficiency, especially at high current density. Consequently, operating temperature should be as high as possible if the life time of fuel cells will not be significantly reduced.

Acknowledgements

The present work was supported by the National Natural Science Fund for Distinguished Young Scholars from the National Natural Science Foundation of China (Nos. 50425620,

50629601) and National Basic Research Program of China (973 Program) (2007CB206902).

References

- [1] J. Larminie, A. Dicks, *Fuel Cell Systems Explained*, 2nd ed., Wiley, Chichester, West Sussex, 2003, pp. 23–24, 30, 141–143.
- [2] P. Costamagna, S. Srinivasan, *J. Power Sources* 102 (2001) 242–252.
- [3] P. Costamagna, S. Srinivasan, *J. Power Sources* 102 (2001) 253–269.
- [4] S. Gamburzev, A.J. Appleby, *J. Power Sources* 107 (2002) 60–66.
- [5] E. Antolini, *J. Appl. Electrochem.* 34 (2004) 563–576.
- [6] R. Chen, T.S. Zhao, *J. Power Sources* 152 (2005) 122–130.
- [7] R.W. Reeve, S. Srinivasan, A.S. Arico, V. Antonucci, *J. Power Sources* 127 (2004) 112–126.
- [8] W.W. Yang, T.S. Zhao, *Electrochim. Acta* 52 (2007) 6125–6140.
- [9] M. Ay, A. Midilli, I. Dince, *Int. J. Energy Res.* 30 (2006) 307–321.
- [10] A. Ishihara, S. Mitsushima, N. Kamiya, K. Ota, *J. Power Sources* 126 (2004) 34–40.
- [11] N. Hotz, M.T. Lee, C.P. Grigoropoulos, S.M. Senn, D. Poulikakos, *Int. J. Heat Mass Transfer* 49 (2006) 2397–2411.
- [12] S.F. Baxter, V.S. Battaglia, R.E. White, *J. Electrochem. Soc.* 146 (1999) 437–447.
- [13] K. Scott, P. Argyropoulos, K. Sundmacher, *J. Power Sources* 477 (1999) 97–110.
- [14] K. Scott, W.M. Taama, P. Argyropoulos, K. Sundmacher, *J. Power Sources* 83 (1999) 204–216.
- [15] Q.S. Fu, *Methods for Thermodynamic Analysis of Energy Systems*, Higher Educational Press, Beijing, 2005, pp. 112–128, 267–279.
- [16] A.A. Kulikovskiy, *Electrochem. Commun.* 5 (2003) 1030–1036.
- [17] B.K. Kho, B. Bae, M.A. Scibioh, J. Lee, H.Y. Ha, *J. Power Sources* 142 (2005) 50–55.
- [18] V. Gurau, H.T. Liu, S. Kakac, *AIChE J.* 44 (1998) 2410–2422.
- [19] A.A. Kulikovskiy, *Electrochem. Commun.* 4 (2002) 939–946.
- [20] EG&G Services Parsons Inc., *Fuel Cell Handbook*, 5th ed., Science Applications Int. Corp. US Department of Energy, National Energy Technology Laboratory, West Virginia, 2000, pp. 6–8 (chapter 2).
- [21] K. Scott, W.M. Taama, S. Kramer, P. Argyropoulos, K. Sundmacher, *Electrochim. Acta* 45 (1999) 945–957.
- [22] T. Berning, *Three dimensional computational analysis of transport phenomena in a PEM fuel cell*, Ph.D. Thesis, University of Victoria, Canada, 2002, p. 84.